Shape Sensing of Medical Devices and Thermal Ablation by means of Fiber Sensors

Capstone Report

Serikbol Sailaubaiuly

Nazarbayev University
Department of Electrical and Computer Engineering
School of Engineering and Digital Sciences

This project report was created on TexStudio editing platform using LaTeX. All the figures were drawn using draw.io online software tool.

NAZARBAYEV UNIVERSITY

Electrical and Computer Engineering
Nazarbayev University
http://www.nu.edu.kz

Title:
Shape Sensing of Medical Devices

Theme:
Fiber Optic sensors

Project Period:
Spring 2024

Project Group:
National Laboratory Astana

Participant(s):
Serikbol Sailaubaiuly

Supervisor(s):
Daniele Tosi

Copies: 1

Page Numbers: 22

Date of Completion:
April 25, 2024

Abstract:

Fiber Optic Shape Sensing brought remarkable advancements to the multitude of different fields. The wide range of its applications has touched the field of medicine, where it can be used in minimally invasive surgeries. FOSS is able to guide surgical instruments and monitor the position, movement and even deformation of organs during the medical procedure. Overall, the objective of shape sensing of medical devices are to improve accuracy, safety, and effectiveness of medical procedures, while minimizing patient discomfort and risk of complications. Additionally, fiber optics are applied for accurate temperature monitoring during laser ablation for the treatment of a cancer. Hence, the objective of this capstone project is to develop and improve new fiber optic shape sensing technologies used in medical devices and cancer treatment, mainly focusing on designing, prototyping and testing a shape sensing of minimally invasive bio-medical devices. Also, corresponding capstone project is aimed to design and analyze the 2D temperature map by means of fiber sensors during the thermal ablation.

Contents

Preface

I would like to express sincere gratitude to my supervisor professor Daniele Tosi. Without his help, my research would not have been of quality nor completed on time. I also thank NU Library for providing students with free access to a large dataset of research papers and articles.

Nazarbayev University, April 25, 2024

Serikbol Sailaubaiuly
<serikbol.sailaubaiuly@nu.edu.kz>

Chapter 1

Introduction

FOSS technology made a breakthroughs and in many engineering fields and Biomedicine and outperformed conventional contact-based shape sensors. Structural health monitoring of buildings, crucial components of airplanes such as wings [1], and tracking the displacement of bio-medical devices without visual contact are several examples of FOSS technology applications [2]. Corresponding technology found to be useful and safer in minimally invasive surgeries. Compared with Fluoroscopy which is widely exploited in surgical interventions and dynamic tracking, FOSS is happened to have more beneficiaries as it does not expose a radiation, offers light-weight and easy installation [2]. Therefore, in order to maintain a minimum damage on the organism and compensate the complicated procedure and tortuosity of paths in cavity, FOSS technologies in minimally invasive surgical needle are critically needed [3].
Another utility of optical fibers is real time temperature sensing during the thermal ablation via Radio Frequency Ablation (RFA), Microwave Ablation (MWA), Laser Interstitial Thermal Therapy (LITT) and High Intensity Focused Ultrasound (HIFU). While all of them have been demonstrated as effective methods of inducing coagulative necrosis within target tumors, Fiber Bragg Grating (FBG) sensors utility has showed high accuracy of ± 0.5 °C during treatment monitoring [4].

Chapter 2

Background

Shape sensors divide into two classifications: conventional shape sensors (CSS) and fiber optic shape sensors (FOSS). Despite the ability of FOSS continuous tracking system, non-contact CSSs, such as cameras, RADARS or LiDARs, can not operate in small size and does not have enough flexibility to bend and curve. Moreover, FOSS are immune to electromagnetic interference and can withstand high temperatures, whereas the performance of CSSs may be negatively affected by the outside temperature and electromagnetic noise in small scales[5].

There exists several techniques that calculates and obtains the shape and position of an optical fiber by analysis of the transmited light behavior. Among them, Brillouin optical time-domain analysis (BOTDA), Rayleigh scattering, Fiber Bragg gratings (FBGs), Optical Backscattering Reflectometry (OBR) are widely used techiques.

The combination of OBR together by tailoring Rayleigh scattering of optical fibers was introduced by Tosi et al. [6]. It is contended that 4 connected fibers to the rigid percutaneous needle provides actual guiding since it displays the dynamic location, shape and accuracy of the insertion [6].

Multi-core optical fibers have also been used for shape sensing. In a study [7], a multi-core optical fiber shape sensing system was proposed for measuring the shape of a curved catheter.

In another study [8], authors propose a new approach comprising FBG based shape sensing, Electromagnetic tracking (EMT) and fluoroscopic imiaging. The results of the research concur with [9], which argue that the precision of shape sensing catheter models are promising.

Likewise, various FBG-based methods were proposed that could improve the accuracy for static and continuous rendering and adequate shape estimation of medical instruments [10, 11, 12].

According to [13], an array of 12 fiber sensors connected to needle was presented and tested on soft-tissue simulant. Gained results show that FBG-based

sensor have high potential and coincides with [8] by claiming that the combined approach of FBG sensors with medical imaging modalities can significantly improve the error accuracy.

Regarding FBGs, for example in thermal ablations, the temperature monitoring is performed in terms of wavelength shift which is one of the most advantageous characteristics. There are primarily two reasons behind such reasoning: first, being an absolute parameter it is more stable and self-calibrating; second, such parameter is loss independent and modal drift [17].

In contrast, distributed optic fiber was suggested as a potential replacement for temperature monitoring techniques used in thermal ablation [14]. It was possible by high-scattering MgO-doped fiber optics which display the whole region of ablation in high resolution.

Nevertheless, the major cause of error and uncertainties in FOSSs is the twisting. [15, 16] propose methods to sense the appearance of twisting and optimize the error accuracy.

There are various methods to ablate the tissue. One of them, Laser ablation (LA) is a thermal ablation technique introduced in the 1980s in the ophthalmologic field and for the treatment of some gastrointestinal and brain tumors. Its main feature is the delivery of energy through small optical fibers (0.3–0.6 mm), in both contact and contactless fashions [18]. RFA allows a rapid (30–120 s) treatment, capable of reaching cytotoxic (>42 °C) and instantaneous cell mortality (>60 °C) temperature values within a few seconds from the start [19]. RFA is highly versatile, and achieves growing success rates in the treatment of solid tumors such as hepatocellular carcinoma, and spinal tumors [20].

Chapter 3

Methodology

3.1 Methods and Procedure of Data Collection

3.1.1 Shape Sensing of Medical Devices

After designing the shape sensing medical device, the algorithm for shape reconstruction of percutaneous needle was modified. It is important to mention that the MATLAB algorithms were initially borrowed from laboratory members and later adjusted accordingly for project purposes. Data was collected via Optical Backscattering Reflectometer LUNA 4600. That is, numerous deformations (strain) and temperature of a needle was tracked with LUNA software. However, due to unexpected breakage of LUNA OBR Software, Micron Optics sensing Instrumentation and Software was introduced to the laboratory which works with Fiber Bragg Grating (FBG) arrays.

3.1.2 Thermal Ablation using Packaged Fiber Sensors

Corresponding complex project consisted of multiple parts. Firstly, the chick embryo chorioallantoic membrane (CAM) samples were cultured. Next, thermal ablation was performed using 980 nm with unfocused light on CAM samples. Four FBG fibers were placed onto the sample in parallel for temperature-sensing purposes. Although mildly related to the initial objective of the project, Brillouin light-scattering spectrometer (BLS) measurements were assembled to assess the elasticity and viscosity of CAM sample before and post 2A, 2.5A ablation.

3.2 Methods and Procedure of Data Analysis

Collected data was imported into MatLab and plotted for further analysis on its strain and temperature parameters.

Chapter 4

Results and Discussions

From the start of the project, all fundamental terms were learned. All activities were held on laboratory. Additional literature reviews were done in regular manner. Appointed PhD student explained the working principle of LUNA OBR4600 and MicronOptics software and their manual was carefully examined. The correct way of splicing the fibers with special machine Fujikura was acquainted. However, fibers have to be cut with special cutting tool for 90 degree cut and thereafter they can be spliced into one using previously mentioned instrument. MatLab code was examined to analyze the gained results by LUNA OBR 4600 software. The project consisted of two parts: construct and analyze the working behavior of percutaneous needle.
In the next step, the focus of the project changed to temperature monitoring through thermal ablation using Laser and Microwave ablations. Results will be examined via MicronOptics software. Unlike LUNA OBR 4600, this time FBG arrays are used instead of distributive sensing optics.

4.1 Literature review

In order to detect serious diseases in early manner, highly effective biosensors became essentially important in diagnostic technologies. Despite the traditional sensors, one of the potentially effective sensors can be an optical fiber LPG biosensor integrated microfluidic chip for glucose detection. According to Yin et al., using optic fiber with a microfluidic chip is a promising combination due to the immunity of optic fiber to the electromagnetic interferences [21] .Long Period Grating (LPG) was inscribed in small-diameter single-mode fiber (SDSMF) and then employed as a sensor. Whilst, layer-by-layer self-assembly technique was used to deposit PEI and PAA films on SDSMF sensor. Next, Microfluidic chip was fabricated, and the LPG SDSMF sensor was integrated inside the chip. Corresponding biosensor works in such a manner that when sensor is encountered with the glu-

cose, the substance reacts with glucose oxidase catalyst and results in a gluconic acid. Consequently, it affects the pH of the resultant mixture, which induces RI and leads to spectra shift of the SDSMF LPG sensor. Thus, the sensor readout component in this biosensor is LPG single-mode optic fiber. It is packaged in a microfluidic chip which offered compactness, low sample consumption and low cost. Following packaged biosensor has two inlets and one outlet serving a function of sample input and output respectively. Moreover, it contained a programmable syringe pump component to control the flow rate. The spiral microfluidic mixing component was placed before the LPG sensors connecting two inlets to mix them homogenously. Likewise, Weidemaier et al., explored a new biosensor to detect a glucose level [22]. Unlike the microfluidic chip, this research combined the fiber optic sensors with GGBP-containing hydrogel matrix attaching it on the glass surface of optic fiber. Afterwards, the optic fiber sensor was put inside the bevel of the needle. Thus, the corresponding GGBP-based packaged biosensor did not contain mixing, waste output components. Nevertheless, the tip of the small diameter optic fiber served as a sample input of corresponding packaged biosensor. Similarly, Endo et al., proposed an optical enzyme sensor system to determine a glucose level [23]. To fabricate a corresponding packaged biosensor, 18-gauge needle was taken. After blocking the hole on the tip of the needle, two holes were made on two opposite sides. Immobilized enzyme membrane was inserted into the self-made hole. Lastly, to set up the packaging of sensor, optic fiber probe including a ruthenium complex was inserted inside the previously mentioned enzyme membrane through another hole. As previously, sample input is a fiber optic, which processes the fluorescence signal gained from ruthenium complex. On the other hand, LPG based optical biosensor can be used to detect Vitamin D. Esposito et al. demonstrated the packaged biosensor coated with a nanoscale layer of graphene oxide for the consequent immobilization of the capture antibody for VitD3 [24]. The LPG double cladding fiber with W-shaped refractive index profile allows to selectively bind the VitD3 close to the fiber boundary. A fabricated biosensor was placed into the Microfluidic system. Additionally, the experimental set up consisted of a flask serving as a sample input. At the same time, syringe pump was connected to control the flow rate of the solution. Whereas Ribaut et al. presented a packaged biosensor of interest for lung cancer (Cytokeration 17) [25]. During the process of packaging biosensor, Tilted Fiber Bragg Gratings (TFBGs) inscribed in the fibers core. Afterwards, they were coated with a gold layer. The tip of the needle was thermo-molded. TFBG-based optic fiber was inserted into the needle and to expose the biosensor to the surrounding environment, a window was laser-cut beyond the packaging tip. The choice of reagents for cancer detection biomarkers in biosensors is determined by the specific biomarkers being targeted, the needed sensitivity, the biosensor technology employed, and the intended application. Monoclonal or polyclonal antibodies can be utilized to bind to specific cancer biomarkers in a sam-

ple. These antibodies are frequently immobilized on the surface of the biosensor, allowing them to collect biomarkers for detection [26]. Cancer biomarkers may be antigens in some circumstances. The production of antigen-antibody complexes, indicating the existence of the biomarker, can be detected using antibodies specific to these biomarkers [27]. Antibodies or other binding molecules can be coupled with enzymes. The enzyme can catalyse a reaction that provides a detectable signal when the antibody binds to the cancer biomarker. This method is commonly used in enzyme-linked immunosorbent tests (ELISAs) [28].

The sensor readout components utilized in a cancer detection biosensor are determined by the biosensing technology used, the target cancer biomarkers, and the required sensitivity and detection limit. Different reading methods have different advantages and disadvantages. Although several alternative methods for early cancer detection have been reported, an electrochemical method is preferred due to its low cost, quick response, simplicity of operation, readily measurable, miniaturization potential, and high sensitivity and selectivity with a lower detection limit [29]. Protein molecular biomarkers are particularly popular due to the wide availability of analytical instrumentation capable of identifying and quantifying proteins in complex biological samples [29].

4.2 Results

Optical fiber sensors can also be packaged into needle for various applications. During this research, few experiments were conducted related to shape sensing devices. First, 4 optic fibers were attached with glue to the nearly 20 cm needle (Fig. 4.1A). Chicken meat and a jelly were used as a phantom to simulate a skin and muscles (Fig. 4.1B).

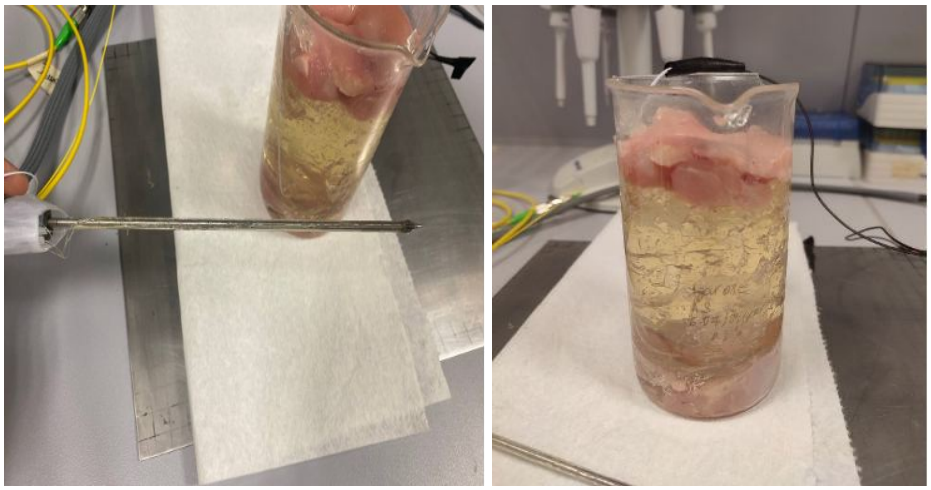

Figure 4.1: A) Shape sensing needle; B) chicken meat and gelatin-based phantom

The very first experiment was conducted to evaluate the strain of the shape sensing device. The results were obtained by Optical Backscatter Reflectometry (OBR) Luna Software and can be seen in Fig. 4.2A. Further, I updated a MATLAB code to plot (Fig. 4.2B), separate strain and temperature parameters and analyze the results (Fig. 4.3A and Fig. 4.3B).

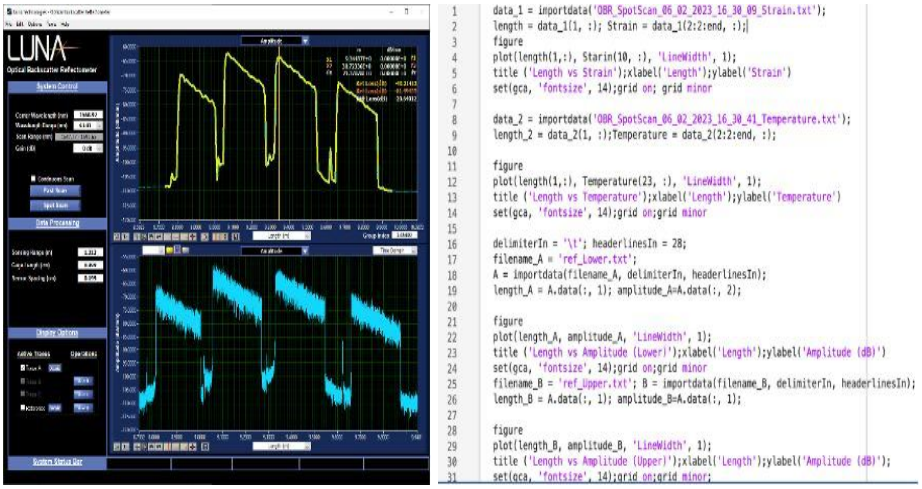

```
data_1 = importdata('OBR_SpotScan_06_02_2023_16_30_09_Strain.txt');
length = data_1(1, :); Strain = data_1(2:2:end, :);
figure
plot(length(1,:), Starin(10, :), 'LineWidth', 1);
title ('Length vs Strain');xlabel('Length');ylabel('Strain')
set(gca, 'fontsize', 14);grid on; grid minor

data_2 = importdata('OBR_SpotScan_06_02_2023_16_30_41_Temperature.txt');
length_2 = data_2(1, :);Temperature = data_2(2:2:end, :);

figure
plot(length(1,:), Temperature(23, :), 'LineWidth', 1);
title ('Length vs Temperature');xlabel('Length');ylabel('Temperature')
set(gca, 'fontsize', 14);grid on;grid minor

delimiterIn = '\t'; headerlinesIn = 28;
filename_A = 'ref_Lower.txt';
A = importdata(filename_A, delimiterIn, headerlinesIn);
length_A = A.data(:, 1); amplitude_A=A.data(:, 2);

figure
plot(length_A, amplitude_A, 'LineWidth', 1);
title ('Length vs Amplitude (Lower)');xlabel('Length');ylabel('Amplitude (dB)')
set(gca, 'fontsize', 14);grid on;grid minor
filename_B = 'ref_Upper.txt'; B = importdata(filename_B, delimiterIn, headerlinesIn);
length_B = A.data(:, 1); amplitude_B=A.data(:, 1);

figure
plot(length_B, amplitude_B, 'LineWidth', 1);
title ('Length vs Amplitude (Upper)');xlabel('Length');ylabel('Amplitude (dB)');
set(gca, 'fontsize', 14);grid on;grid minor;
```

Figure 4.2: A) OBR software as the measurement is being done; B) Updated MATLAB code to obtain strain/ temperature parameters

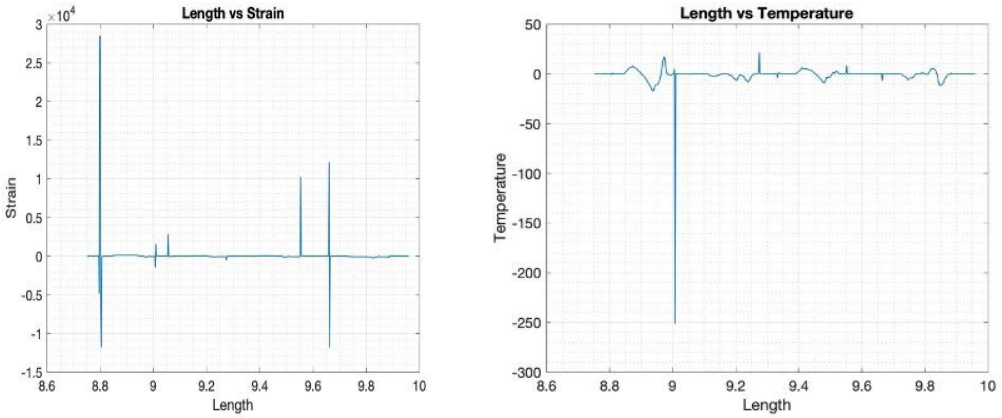

Figure 4.3: (A) Length vs Strain graph; (B) Length vs Temperature graph

The aim of the second experiment was to test the sensitivity of fiber optics to temperature. To do that, 20 cm needle was heated and put on the chicken meat as it can be seen in Fig. 4A. In order to reach a high temperature, LeanFa Hybrid Generator was used (Fig. 5A). The shape sensing needle was connected to the positive charge, while the metal plate under the chicken meat was connected to negative charge of the LeanFa Hybrid Generator (Fig. 5B). After setting needed

configurations the edge of needle was heated to nearly 100 degrees Celsius. After 15 minutes the outer layer of chicken was slightly burned as it can be seen in Fig. 4B.

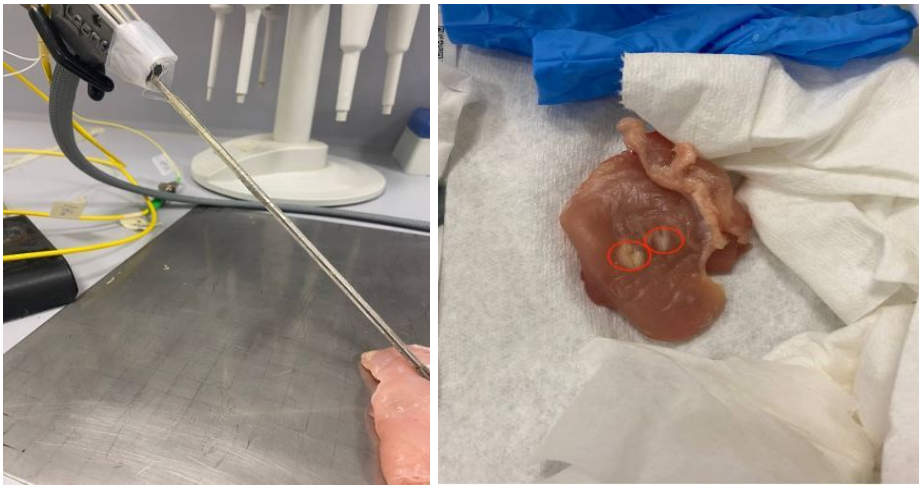

Figure 4.4: Sensor embedded into the needle applied to chicken meat (A); Chicken meat after heating shape sensing needle (B)

Figure 4.5: LeanFa Hybrid Generator (A) and positive and negative probes (B)

Figure 4.6: Luna results displaying temperature rise gained by heating a chicken meat

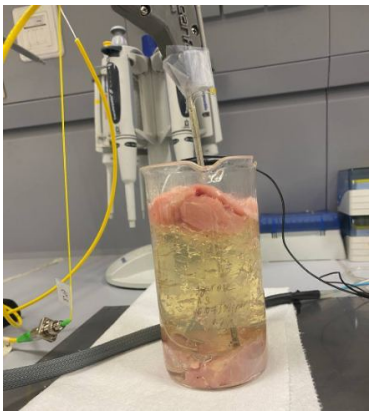

Figure 4.7: Experimental Setup showing needle with the packaged sensor inside the phantom

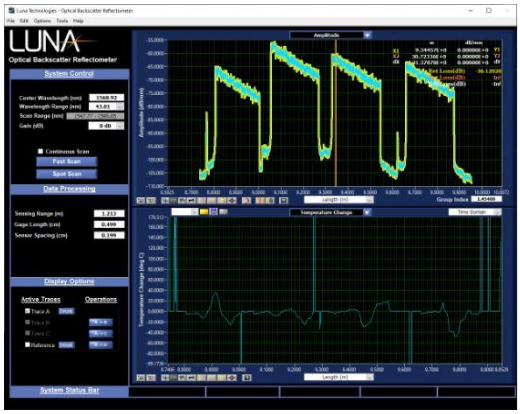

Figure 4.8: Luna results displaying temperature on biosensor gained by heating phantom

Because of sudden breakage of LUNA OBR software, the focus of the project changed from conducting more experiments to analyzing the obtained data and writing a new MATLAB code measure its Strain parameters. Currently, the first version of the MATLAB algorithm can present the Amplitude as it can be seen in Fig. 4.9

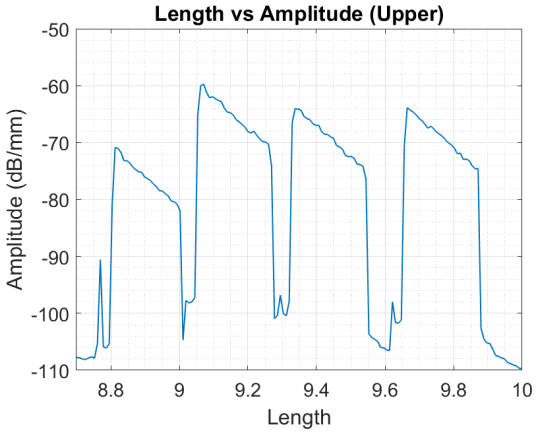

Figure 4.9: Length vs Amplitude

Second version of code clearly depicts the strain measurement of each fiber separately, which is shown in Fig. 4.10.

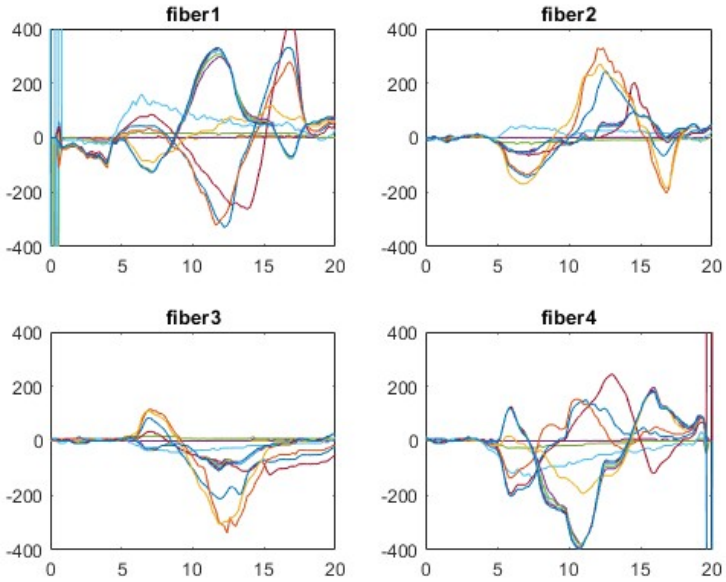

Figure 4.10: Strain measurement of corresponding fibers

Last semester was devoted to another research line, thermal ablation. Unlike previous experiments, a living organism was cultured to implement the experiments on. That is, the Chick Embryo Chorioallantoic membrane (CAM) model was prepared in order to examine the thermal ablation. Four fibers were placed 2 mm from each other along the ablated area (Fig. 4.11). 980 nm unfocused laser was used for ablation in order to increase the spot size. During the experiment, the

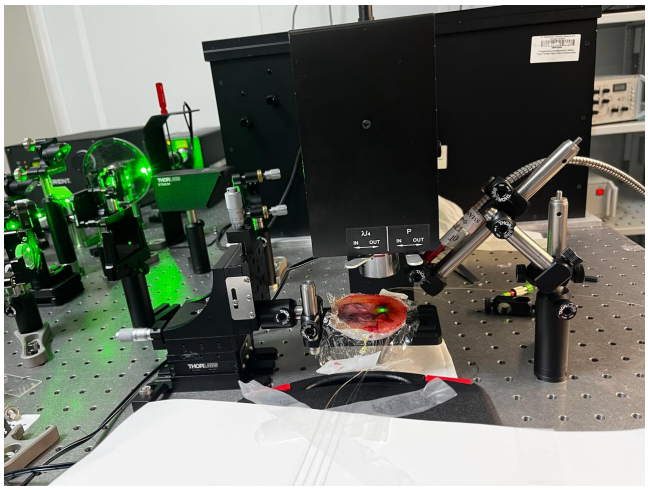

Figure 4.11: Experimental setup for Laser Ablation

BLS measurements were taken to assess the viscosity of ablated area at different stages (Fig. 4.12).

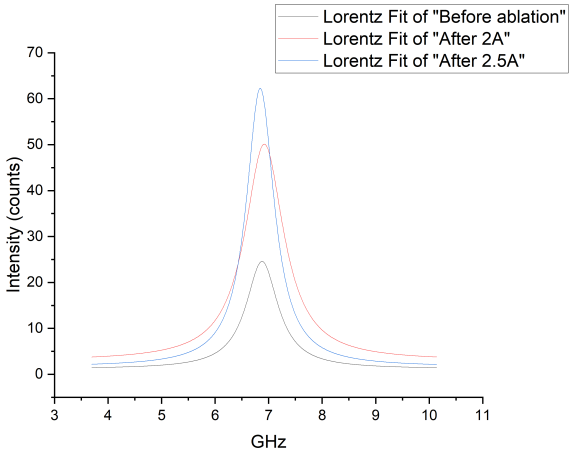

Figure 4.12: BLS measurements

As a result, thermal map was obtained via MATLAB algorithm that can be seen in Fig. 4.13.

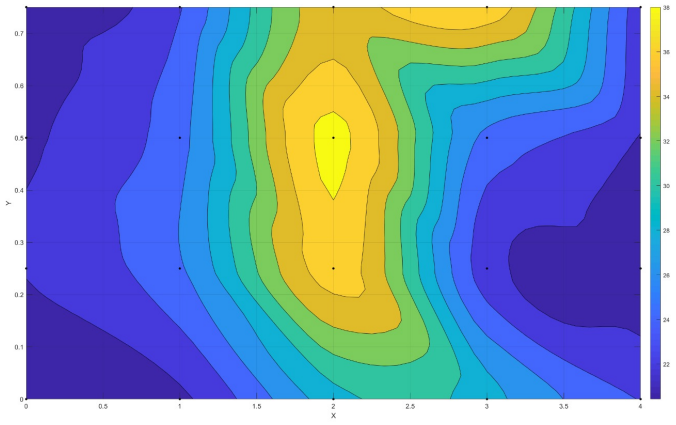

Figure 4.13: 2D Thermal Map obtained via MATLAB

4.3 Discussions

The first experiment was focused to test the strain of the needle. Corresponding MATLAB code was written to obtain detailed graphs for every instance. Chicken meat and gelatin-based phantom was decided to be appropriate for current project. Second experiment was more complex as it included new equipment LeanFA Hybrid Generator that uses RF waves to heat the very edge of the needle. Fig. 4.7 illustrates the experimental setup with shape sensing needle inside the phantom. It is worth noting that first fifteen sample scans were taken to measure strain parameters and the rest scans was taken to measure temperature rise. Pre-experimental results were promising, though the results of the actual experiment were controversial. It can be seen from Luna measurements in Fig. 4.6 (pre-experiment) and Fig. 4.8 (actual experiment). While in pre-experimental case all four fibers displayed similar temperature values around 80 degrees, actual experiment results were different in all four fibers. Figures 10 demonstrates the strain measurements between [400,-400] um and conversely proportional patterns can be explored between fiber 1 (upper) and fiber 4 (lower), fiber 2 (left) and fiber 3 (right). Regarding Thermal Ablation Project, corresponding experiment was conducted to test the setup and anticipate the potential problems. For instance, it can be noticed that the peak temperature at ablated area was around 40 °C, though it was expected to reach 60 °C. It was assumed that the CAM model does not efficiently absorb the light. Hence, coating with nanoparticles such as gold was offered as a solution to increase the absorption coefficient. Additionally, same age of CAM models were assumed to be used to increase the accuracy of experiment. In future, it is planned to conduct an experiment using microwave and radio frequency ablation and compare their efficiency.

Chapter 5

Conclusion

Literature review was done in the field of packaged biosensors. More precisely, the review of main components of packaged biosensors was made. The way how biosensors were packaged inside the chips, needles, Sample Input, Sensor Readouts were discussed. Lastly, the evaluation of strain and temperature parameters of Shape Sensing needle was made. After careful consideration, it was suggested that the reasons of unexpected results can be low conductivity of gelatin-based phantom and low Power set in LeanFa Hybrid Generator. It is important to note that the sudden breakage of LUNA OBR Software significantly halted the progress of the project. After obtaining datasets, new MATLAB algorithm was constructed to closely represent the strain and temperature measurements. Further work will be conducted via MicronOptics software and due to the reason that the current Percutaneous device fibers are incompatible with new signal interrogator, the project will be started afresh. Regarding Thermal Ablation Project, gained results are acceptable for the first trial and can be further improved. Future related experiments are expected to be conducted with the arrival of appropriate FBG sensors.

Bibliography

[1] Zhen Ma and Xiyuan Chen. "Fiber Bragg Gratings Sensors for Aircraft Wing Shape Measurement: Recent Applications and Technical Analysis". In: *Sensors* 19.1 (2019). ISSN: 1424-8220. DOI: 10.3390/s19010055. URL: https://www.mdpi.com/1424-8220/19/1/55.

[2] Ignazio Floris et al. "Fiber Optic Shape Sensors: A comprehensive review". In: *Optics and Lasers in Engineering* 139 (2021), p. 106508. ISSN: 0143-8166. DOI: https://doi.org/10.1016/j.optlaseng.2020.106508. URL: https://www.sciencedirect.com/science/article/pii/S0143816620319461.

[3] Aizhan Issatayeva et al. "Design and analysis of a fiber-optic sensing system for shape reconstruction of a minimally invasive surgical needle". In: *Scientific Reports* 11.1 (2021), p. 8609.

[4] Rory Geoghegan et al. "Methods of monitoring thermal ablation of soft tissue tumors – A comprehensive review". In: *Medical Physics* 49.2 (2022), pp. 769–791. DOI: https://doi.org/10.1002/mp.15439. eprint: https://aapm.onlinelibrary.wiley.com/doi/pdf/10.1002/mp.15439. URL: https://aapm.onlinelibrary.wiley.com/doi/abs/10.1002/mp.15439.

[5] Moe Amanzadeh et al. "Recent developments in fibre optic shape sensing". In: *Measurement* 128 (2018), pp. 119–137.

[6] Daniele Tosi et al. "Enhanced Backscattering Optical Fiber Distributed Sensors: Tutorial and Review". In: *IEEE Sensors Journal* 21.11 (2021), pp. 12667–12678. DOI: 10.1109/JSEN.2020.3010572.

[7] Fouzia Khan et al. "Multi-Core Optical Fibers With Bragg Gratings as Shape Sensor for Flexible Medical Instruments". In: *IEEE Sensors Journal* 19.14 (2019), pp. 5878–5884. DOI: 10.1109/JSEN.2019.2905010.

[8] Xuan Thao Ha et al. "Robust Catheter Tracking by Fusing Electromagnetic Tracking, Fiber Bragg Grating and Sparse Fluoroscopic Images". In: *IEEE Sensors Journal* 21.20 (2021), pp. 23422–23434. DOI: 10.1109/JSEN.2021.3107036.

[9] Sonja Jäckle et al. “Fiber optical shape sensing of flexible instruments for endovascular navigation”. In: *International journal of computer assisted radiology and surgery* 14 (2019), pp. 2137–2145.

[10] Omar Al-Ahmad et al. “Improved FBG-Based Shape Sensing Methods for Vascular Catheterization Treatment”. In: *IEEE Robotics and Automation Letters* 5.3 (2020), pp. 4687–4694. DOI: 10.1109/LRA.2020.3003291.

[11] Chaojiang He et al. “Optical fiber shape sensing of flexible medical instruments with temperature compensation”. In: *Optical Fiber Technology* 74 (2022), p. 103123. ISSN: 1068-5200. DOI: https://doi.org/10.1016/j.yofte.2022.103123. URL: https://www.sciencedirect.com/science/article/pii/S1068520022003066.

[12] LeiFeng Zhang et al. “A New Method For Fiber Bragg Grating Based Needle Shape Sensing Calibration”. In: *2019 IEEE International Conference on Robotics and Biomimetics (ROBIO)*. 2019, pp. 1953–1958. DOI: 10.1109/ROBIO49542.2019.8961717.

[13] Roy J. Roesthuis et al. “Three-Dimensional Needle Shape Reconstruction Using an Array of Fiber Bragg Grating Sensors”. In: *IEEE/ASME Transactions on Mechatronics* 19.4 (2014), pp. 1115–1126. DOI: 10.1109/TMECH.2013.2269836.

[14] Aidana Beisenova et al. “Distributed Sensing Network Enabled by High-Scattering MgO-Doped Optical Fibers for 3D Temperature Monitoring of Thermal Ablation in Liver Phantom”. In: *Sensors* 21.3 (2021). ISSN: 1424-8220. DOI: 10.3390/s21030828. URL: https://www.mdpi.com/1424-8220/21/3/828.

[15] Qingqing Guo et al. “Twist Angle Compensation for Three Dimensional Real-Time Shape Sensing Method Based on Multi-Core Optical Fiber”. In: *2020 12th International Conference on Measuring Technology and Mechatronics Automation (ICMTMA)*. 2020, pp. 402–406. DOI: 10.1109/ICMTMA50254.2020.00094.

[16] Ignazio Floris et al. “Twisting measurement and compensation of optical shape sensor based on spun multicore fiber”. In: *Mechanical Systems and Signal Processing* 140 (2020), p. 106700. ISSN: 0888-3270. DOI: https://doi.org/10.1016/j.ymssp.2020.106700. URL: https://www.sciencedirect.com/science/article/pii/S0888327020300868.

[17] Manish Mishra and Prasant Kumar Sahu. “Fiber Bragg Gratings in Healthcare Applications: A Review”. In: *IETE Technical Review* 40.2 (2023), pp. 202–219. DOI: 10.1080/02564602.2022.2069608. eprint: https://doi.org/10.1080/02564602.2022.2069608. URL: https://doi.org/10.1080/02564602.2022.2069608.

[18] Federica Morra et al. “Spatially resolved thermometry during laser ablation in tissues: Distributed and quasi-distributed fiber optic-based sensing”. In: *Optical Fiber Technology* 58 (2020), p. 102295. ISSN: 1068-5200. DOI: https://doi.org/10.1016/j.yofte.2020.102295. URL: https://www.sciencedirect.com/science/article/pii/S1068520020302856.

[19] Akbota Sametova et al. “Optical Fiber Distributed Sensing Network for Thermal Mapping in Radiofrequency Ablation Neighboring a Blood Vessel”. In: *Biosensors* 12.12 (2022). ISSN: 2079-6374. DOI: 10.3390/bios12121150. URL: https://www.mdpi.com/2079-6374/12/12/1150.

[20] Akbota Sametova et al. “Fiber-Optic Distributed Sensing Network for Thermal Mapping of Gold Nanoparticles-Mediated Radiofrequency Ablation”. In: *Biosensors* 12.5 (2022). ISSN: 2079-6374. DOI: 10.3390/bios12050352. URL: https://www.mdpi.com/2079-6374/12/5/352.

[21] Ming jie Yin et al. “Optical fiber LPG biosensor integrated microfluidic chip for ultrasensitive glucose detection”. In: *Biomed. Opt. Express* 7.5 (2016), pp. 2067–2077. DOI: 10.1364/BOE.7.002067. URL: https://opg.optica.org/boe/abstract.cfm?URI=boe-7-5-2067.

[22] Kristin Weidemaier et al. “Multi-day pre-clinical demonstration of glucose/-galactose binding protein-based fiber optic sensor”. In: *Biosensors and Bioelectronics* 26.10 (2011), pp. 4117–4123. ISSN: 0956-5663. DOI: https://doi.org/10.1016/j.bios.2011.04.007. URL: https://www.sciencedirect.com/science/article/pii/S095656631100203X.

[23] Hideaki Endo et al. “A needle-type optical enzyme sensor system for determining glucose levels in fish blood”. In: *Analytica Chimica Acta* 573-574 (2006). Instrumental Methods of Analysis -IMA 2005, pp. 117–124. ISSN: 0003-2670. DOI: https://doi.org/10.1016/j.aca.2006.04.068. URL: https://www.sciencedirect.com/science/article/pii/S0003267006008981.

[24] Flavio Esposito et al. “Label-free detection of vitamin D by optical biosensing based on long period fiber grating”. In: *Sensors and Actuators B: Chemical* 347 (2021), p. 130637. ISSN: 0925-4005. DOI: https://doi.org/10.1016/j.snb.2021.130637. URL: https://www.sciencedirect.com/science/article/pii/S0925400521012053.

[25] Clotilde Ribaut et al. “Cancer biomarker sensing using packaged plasmonic optical fiber gratings: Towards in vivo diagnosis”. In: *Biosensors and Bioelectronics* 92 (2017), pp. 449–456. ISSN: 0956-5663. DOI: https://doi.org/10.1016/j.bios.2016.10.081. URL: https://www.sciencedirect.com/science/article/pii/S0956566316311216.

[26] James F. Rusling et al. “Low Cost 3D-Printed Biosensor Arrays for Protein-based Cancer Diagnostics based on Electrochemiluminescence”. In: *SCITEPRESS* 1 (2016), pp. 17–22. ISSN: 0956-5663. DOI: DOI:10.5220/0005649000170022. URL: https://www.scitepress.org/Papers/2016/56490/56490.pdf.

[27] Khalid Ibrahimi et al. “Enhanced Design and Analysis of the Microcantilever-Based Bio-Sensor to Detect Carcinoembryonic Antigen Tumor Biomarkers”. In: *Computer Assisted Methods in Engineering and Science* 30.3 (2023), pp. 347–367. ISSN: 2956-5839. DOI: 10.24423/cames.654. URL: https://cames.ippt.pan.pl/index.php/cames/article/view/654.

[28] Kawde Abdel-Nasser et al. “Enhanced Design and Analysis of the Microcantilever-Based Bio-Sensor to Detect Carcinoembryonic Antigen Tumor Biomarkers”. In: *American Journal of Bimedical Sciences* 2.1 (2009), pp. 23–32. ISSN: 1937-9080. DOI: doi:10.5099/aj100100023. URL: https://www.researchgate.net/profile/Abdel-Nasser-Kawde/publication/228785369_Moving_Enzyme-Linked_ImmunoSorbent_Assay_to_the_Point-of-Care_Dry-Reagent_Strip_Biosensors/links/0c9605176cb64106db000000/Moving-Enzyme-Linked-ImmunoSorbent-Assay-to-the-Point-of-Care-Dry-Reagent-Strip-Biosensors.pdf.

[29] M.R. Hasan et al. “Recent development in electrochemical biosensors for cancer biomarkers detection”. In: *Biosensors and Bioelectronics: X* 8 (2021), p. 100075. ISSN: 2590-1370. DOI: https://doi.org/10.1016/j.biosx.2021.100075. URL: https://www.sciencedirect.com/science/article/pii/S259013702100011X.

Appendix A

MATLAB code for getting Amplitude and Strain

```
% close all figures
close all
% remove items from workspace
clear
% clear command window
clc

data_1 = importdata('OBR_SpotScan08_08_2023_14_56_21_Strain.txt');
length = data_1(1, :);
Strain = data_1(2:2:end, :);

%
%
%
%
Strain_new = Strain;
Strain_new(:, 1:25) = 0;
Strain_new(:, 127:150) = 0;

subplot(2,2,1)
fiber1 = Strain_new(:, 25:125);
length_new = 0:0.2:20;
plot(length_new, fiber1)
ylim ([-400 400])
title("fiber1")
```

```
subplot(2,2,2)
fiber2 = Strain_new(:, 158:258);
length_new = 0:0.2:20;
plot(length_new, fiber2)
ylim ([-400 400])
title("fiber2")

subplot(2,2,3)
fiber3 = Strain_new(:, 295:395);
length_new = 0:0.2:20;
plot(length_new, fiber3)
ylim ([-400 400])
title("fiber3")

subplot(2,2,4)
fiber4 = Strain_new(:, 466:566);
length_new = 0:0.2:20;
plot(length_new, fiber4)
ylim ([-400 400])
title("fiber4")

delimiterIn = '\t';
headerlinesIn = 28;

filename_B = 'ref1_Upper.txt';
B = importdata(filename_B, delimiterIn, headerlinesIn/2);
length_B = B.data(:, 1);
amplitude_B=B.data(:, 2);

figure
plot(length_B, amplitude_B, 'LineWidth', 1);
title ('Length vs Amplitude (Upper)')
xlabel('Length')
ylabel('Amplitude (dB/mm)')
set(gca, 'fontsize', 14);
xlim([8.7 10]);
grid on
grid minor
```

textbfExample of code to obtain Amplitude (dB/mm) and Strain

```
close all
clear all
clc

L = 0.2;  % length of each section along the needle or sensors spacing in cm
z = 0:L:20; % needle length in cm
interval = length(z);
d = 0.25; %diameter of the needle in cm

% N_start = 1;
% N_stop = 11; % number of txt files
% strain_column = 8; % in txt
% length_column = 2; % in txt

% Extract strain values from txt files
% for ii = N_start:N_stop
% delimiterIn = '\t';
% headerlinesIn = 28;
% Filename = 'ref1_Lower.txt';
A = importdata('OBR_SpotScan08_08_2023_14_56_21_Strain.txt');
Length = A(1, :);
length_new = 0:0.2:20;
Strain = A(2:2:end, :);
% Define the ranges you want to extract
ranges = [30:125, 158:258, 295:395, 466:563];

% Create an array of zeros with the same size as Strain
zeroStrain = zeros(size(Strain));

% Assign the strain values within the specified ranges to zeroStrain
zeroStrain(:, ranges) = Strain(:, ranges);
%     Reference = strcat('ref',num2str(ii-1),'.txt');
%
%     B = importdata(Reference); % References are used only in needle calibrati
%     Ref(ii,:) = B;
% end


% The whole graph for all fibers
```

```
figure
plot(Length, zeroStrain)
xlabel('Length (m)','FontSize', 14)
ylabel('Strain (\mu\epsilon)','FontSize', 14)
set(gca,'fontsize',14)

figure
fiber1 = zeroStrain(:, 26:126);
plot(length_new, fiber1)
%ylim ([-400 400])
title("Upper fiber (1)")

figure
fiber2 = zeroStrain(:, 159:259);
plot(length_new, fiber2)
%ylim ([-400 400])
title("Left fiber (2)")

figure
fiber3 = zeroStrain(:, 296:396);
plot(length_new, fiber3)
%ylim ([-400 400])
title("Right fiber (3)")

figure
fiber4 = zeroStrain(:, 464:564);
plot(length_new, fiber4)
%ylim ([-400 400])
title("Lower fiber (4)")
```

Shape sensing without the application of correction coefficients